JOURNAL OF NEUROTRAUMA 28:95–104 (January 2011)
© Mary Ann Liebert, Inc.
DOI: 10.1089/neu.2010.1513

A Multi-Mode Shock Tube for Investigation of Blast-Induced Traumatic Brain Injury

Dexter V. Reneer,[1,2] Richard D. Hisel,[6] Joshua M. Hoffman,[3] Richard J. Kryscio,[4,5] Braden T. Lusk,[3] and James W. Geddes[1,2]

Abstract

Blast-induced mild traumatic brain injury (bTBI) has become increasingly common in recent military conflicts. The mechanisms by which non-impact blast exposure results in bTBI are incompletely understood. Current small animal bTBI models predominantly utilize compressed air-driven membrane rupture as their blast wave source, while large animal models use chemical explosives. The pressure-time signature of each blast mode is unique, making it difficult to evaluate the contributions of the different components of the blast wave to bTBI when using a single blast source. We utilized a multi-mode shock tube, the McMillan blast device, capable of utilizing compressed air- and compressed helium-driven membrane rupture, and the explosives oxyhydrogen and cyclotrimethylenetrinitramine (RDX, the primary component of C-4 plastic explosives) as the driving source. At similar maximal blast overpressures, the positive pressure phase of compressed air-driven blasts was longer, and the positive impulse was greater, than those observed for shockwaves produced by other driving sources. Helium-driven shockwaves more closely resembled RDX blasts, but by displacing air created a hypoxic environment within the shock tube. Pressure-time traces from oxyhydrogen-driven shockwaves were very similar those produced by RDX, although they resulted in elevated carbon monoxide levels due to combustion of the polyethylene bag used to contain the gases within the shock tube prior to detonation. Rats exposed to compressed air-driven blasts had more pronounced vascular damage than those exposed to oxyhydrogen-driven blasts of the same peak overpressure, indicating that differences in blast wave characteristics other than peak overpressure may influence the extent of bTBI. Use of this multi-mode shock tube in small animal models will enable comparison of the extent of brain injury with the pressure-time signature produced using each blast mode, facilitating evaluation of the blast wave components contributing to bTBI.

Key words: helium; overpressure; oxyhydrogen; pressure-time signature; RDX

Introduction

Blast-induced mild traumatic brain injury (bTBI) has become increasingly common in current conflicts due to the increased use of improvised explosive devices (IEDs), as well as advances in body armor and medical care that result in improved survivability of blast injuries (Armonda et al., 2006; Cernak and Noble-Haeusslein, 2010; Elder and Cristian, 2009; Hoge et al., 2008). The mechanisms by which non-impact blast exposure results in bTBI are incompletely understood, and are the subject of much current investigation using both large- and small-animal models. While the majority of large-animal models of blast injury utilize chemical explosives as the source of the blast wave (Bauman et al., 2009; Garner et al., 2009; Saljo et al., 2008), most small-animal studies utilize compressed air-driven shock tubes (Cernak et al., 2001; Chavko et al., 2007; Elder and Cristian, 2009).

Blast waves are created by the very rapid conversion of a solid or liquid into a gas (Mayorga, 1997). The rapid expansion of the gas compresses the surrounding air to create a blast overpressure wave, which then decays exponentially and is followed by a relative vacuum, the underpressure wave. The pressure-time trace of an ideal blast wave is described by a Friedlander waveform (Fig. 1; Baker, 1973).

Currently there is uncertainty regarding the contribution of various components of a blast wave to bTBI. Most small-animal blast injury studies examine the role of blast overpressure on test subjects by using peak overpressure as the

[1]Spinal Cord and Brain Injury Research Center, [2]Department of Anatomy and Neurobiology, [3]Department of Mining Engineering, [4]Department of Biostatistics, and [5]Department of Statistics, University of Kentucky, Lexington, Kentucky.
[6]GLR Enterprises, L.L.C., Nicholasville, Kentucky.

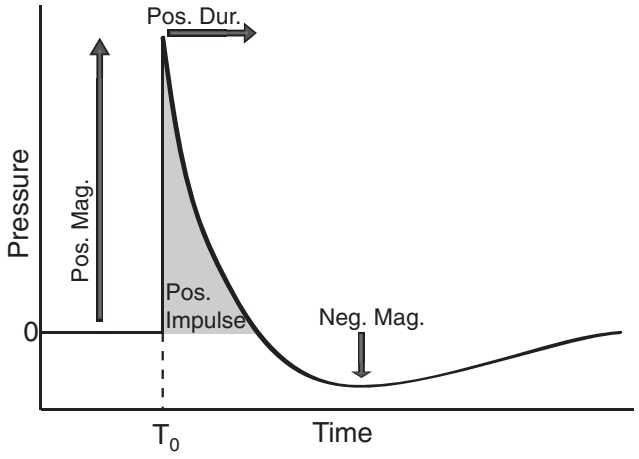

FIG. 1. The Friedlander wave. The Friedlander wave describes an ideal blast from a spherical source in an open environment. T_0 is the time at which the pressure began to rise above ambient pressure. Positive magnitude (Pos. Mag.) is the difference between peak pressure and ambient pressure. Positive duration (Pos. Dur.) is the time between T_0 and when the pressure goes below ambient pressure. Positive impulse (Pos. Impulse) is the integral of the pressure-time trace during the positive phase. Negative magnitude (Neg. Mag.) is the difference between ambient and peak negative pressure.

measure of blast wave intensity (Cernak et al., 2001; Chavko et al., 2006, 2007; Long et al., 2009; Saljo et al., 2009). However, the peak overpressures used to induce bTBI have varied widely, ranging from 20 kPa to 340 kPa for whole-body exposure in rats (Cernak et al., 2001; Moochhala et al., 2004), 150 kPa for head-only exposure (Cheng et al., 2010), and up to 10,000 kPa for direct brain exposure (Kato et al., 2007). In addition to maximal overpressure, the damaging effects of a blast wave may also depend on the duration of the positive pressure wave, as well as a contribution from the negative pressure wave (Gruss, 2006; Marks, 2002; Zhang et al., 1996). These characteristics are determined not only by the blast source itself, but also by the distance from the blast and the effects of reflections from walls or in a confined area such as a vehicle.

To examine the contribution of various components of the blast wave to bTBI, we designed and constructed the McMillan blast device (MBD; Fig. 2; the McMillan blast device was named in honor of United States Army Cpl. William L. McMillan, III, of Lexington, Kentucky, who gave his life in service to his country on July 8, 2008 after his patrol was struck by an improvised explosive device). This is a shock tube similar in design to the shock tube at the Walter Reed Army Institute of Research and Naval Medical Research Center in Silver Spring, Maryland (Chavko et al., 2006; Elsayed, 1997; Long et al., 2009). The MBD is capable of utilizing four different modes to produce a shock wave: compressed air, compressed helium, oxyhydrogen, and RDX (cyclotrimethylenetrinitramine, the main explosive component of C-4 plastic explosives). Each blast mode results in a distinct pressure-time trace. The principal goal of this study was to characterize the various blast modes produced by the MBD by evaluating six parameters of the resultant blast wave and pressure-time trace: shock wave velocity, positive phase magnitude, positive phase duration, positive phase impulse, negative phase magnitude, and the impulse difference between reflected and free-field pressures. Another goal of this study was to begin to examine the extent of brain injury produced by each of the blast modes at similar peak overpressures. This will allow evaluation of the potential contribution of different components of the blast wave to bTBI in small-animal models.

Methods

McMillan blast device

The MBD (Fig. 2) consists of a cylindrical steel tube, 12-inch internal diameter, separated into a 19-ft. expansion chamber and a 2.5-ft compression chamber. When in compressed air- or compressed helium-driven mode, a 10-mil-thick (0.254 mm) biaxially-oriented polyethylene terephthalate (Mylar®) membrane separates the two chambers (Mylar A; Tekra Corp., New Berlin, WI; Fig. 2B). In compressed gas-driven modes the compression chamber is filled with either compressed air obtained from an on-site air compressor or industrial grade compressed helium (Scott-Gross Company, Inc., Lexington, KY), until the Mylar membrane spontaneously ruptures (compressed air-driven mode), or is manually ruptured at the desired load pressure (compressed helium-driven mode) by a 4-point blade affixed to a pneumatic cylinder.

In the oxyhydrogen-driven mode, a steel manifold was placed between the expansion and compression chambers (Fig. 2C). The manifold contained tubing for oxygen and hydrogen leading to a central flange on the side facing the expansion chamber. A thin polyethylene bag was attached to the flange and filled with a 2:1 mixture of gaseous hydrogen and oxygen. The oxyhydrogen mixture was ignited by a small cordite charge (Winchester Ammunition #209 ShotShell Primer; Olin Corporation, Clayton, MO).

In RDX-driven mode (not shown), an electric detonator (RockStar Electric Detonator; Austin Powder Co., Cleveland, OH) was embedded in 1.4 g of RDX (desensitized; Accurate Energetic Systems, L.L.C., McEwen, TN). The two were then wrapped in a thin layer of latex and secured with electrical tape to create a single explosive unit, which was positioned in the center of the vertical axis of the expansion chamber 6 inches from the steel manifold. The explosive unit was detonated using an electronic blasting machine (Scorpion HB-SBS; E.I.T. Corp, Sunbury, PA).

For each mode, the shock wave was recorded by face-on, reflected pressure (PCB model #113A24; PCB Piezotronics, Inc., Depew, NY; Fig. 2D), and free-field averaging sensors (model #137A22; Fig. 2E). The free-field sensor was positioned inside the shock tube with the sensing element located 10 inches from the open end and the point facing towards the blast source. The reflected pressure sensor was installed in the dorsal surface of a solid polyurethane rat model (Fig. 2D). The model was then installed with the dorsal surface of the rat positioned such that the sensor faced toward the blast source. This sensor was also located inside the blast tube, 10 inches from the open end of the expansion chamber. During shock-wave velocity recordings, two free-field sensors were positioned inside the tube, separated by a distance of 12 inches. Data from each sensor was routed through a line signal con-

FIG. 2. The McMillan blast device (MBD). (**A**) Photo of the entire device. The flanges at the adjacent edges between the compression and expansion chambers are lined with silicone gaskets that seal around a Mylar membrane. In compressed air- or compressed helium-driven mode, the Mylar membrane is naturally ruptured or is ruptured by a 4-point blade affixed to a pneumatic cylinder that is designed to induce complete membrane failure at a pre-determined pressure in the compression chamber. (**B**) The Mylar sheet is inserted between the compression and expansion chambers of the MBD. (**C**) For the explosive-driven modes (oxyhydrogen or RDX) a blast plate is inserted between the compression and expansion chambers. The plate contains a manifold for the hydrogen and oxygen, which flow into a flange facing the expansion chamber. The polyethylene bag is inserted over the flange and filled with the hydrogen and oxygen. (**D**) The reflected (face-on) pressure sensor (PCB model #113A24) embedded in the dorsal surface of the polyurethane rat model. (**E**) The free field (side-on) sensor (PCB model #137A22). (**F**) The anesthetized rat is fitted with a Kevlar vest (not shown) and inserted into a mesh netting support. This is then loaded into a shock tube insert. The netting is tightened and securely fastened to prevent rotational movement of the head during blast exposure. The insert is placed into a cutout in the MBD such that the rat is positioned laterally within the expansion chamber of the shock tube approximately 1 foot from the open end, with the left side of the rat facing the blast source. Following blast exposure, the insert is rapidly removed and the rat is removed from the netting (RDX, cyclotrimethylenetrinitramine).

ditioner (PCB model #482A21) before being captured by a digital storage oscilloscope (MicroTrap VOD/Data Recorder; MREL Group of Companies, Ltd., Kingston, Ontario, Canada). Data were analyzed using MicroTrap 7.2 (MREL), DPlot v2.2.5.7, and Microsoft Excel 2007. Data were graphed using DPlot and PRISM v4.0.

Blast wave parameters and data analysis

The amount of compressed air, compressed helium, oxyhydrogen, or RDX was adjusted so that the peak overpressure in each blast was approximately 120 kPa. Due to the oscillating nature of the pressure-time trace, a curve fit was utilized to

determine the time at which the blast trace crossed the ambient pressure line (0 kPa). An eighth-order least squares polynomial was found to be a superior fit and was fitted to the data using DPlot, beginning at the peak pressure reported by the sensor (Fig. 3). Shockwave velocity was calculated based on the time required for the shockwave to travel between the two free-field sensors spaced 12 inches apart. Negative phase magnitude was the minimum value of the eighth-order curve fit for a given pressure-time trace. Positive phase duration was calculated as the amount of time between the first substantial rise in pressure recorded for a given blast wave trace (T_0), and the time at which the eighth-order curve fit crossed back over the ambient pressure line (0 kPa). Positive impulse is the integral of the pressure-time trace, and is related to the linear kinetic energy contained in the blast wave. The impulse difference between reflected and free-field pressures (Δ Impulse), also a measure of kinetic energy, was calculated by subtracting the positive impulse of the free-field sensor from that of the reflected pressure sensor (Benzinger et al., 2009).

Gas content following blast

Using a gas other than air to fill the compression chamber of the MBD, or the combustion of explosives, may create a hypoxic environment that could compound injury data. Oxygen and carbon monoxide content were measured using a

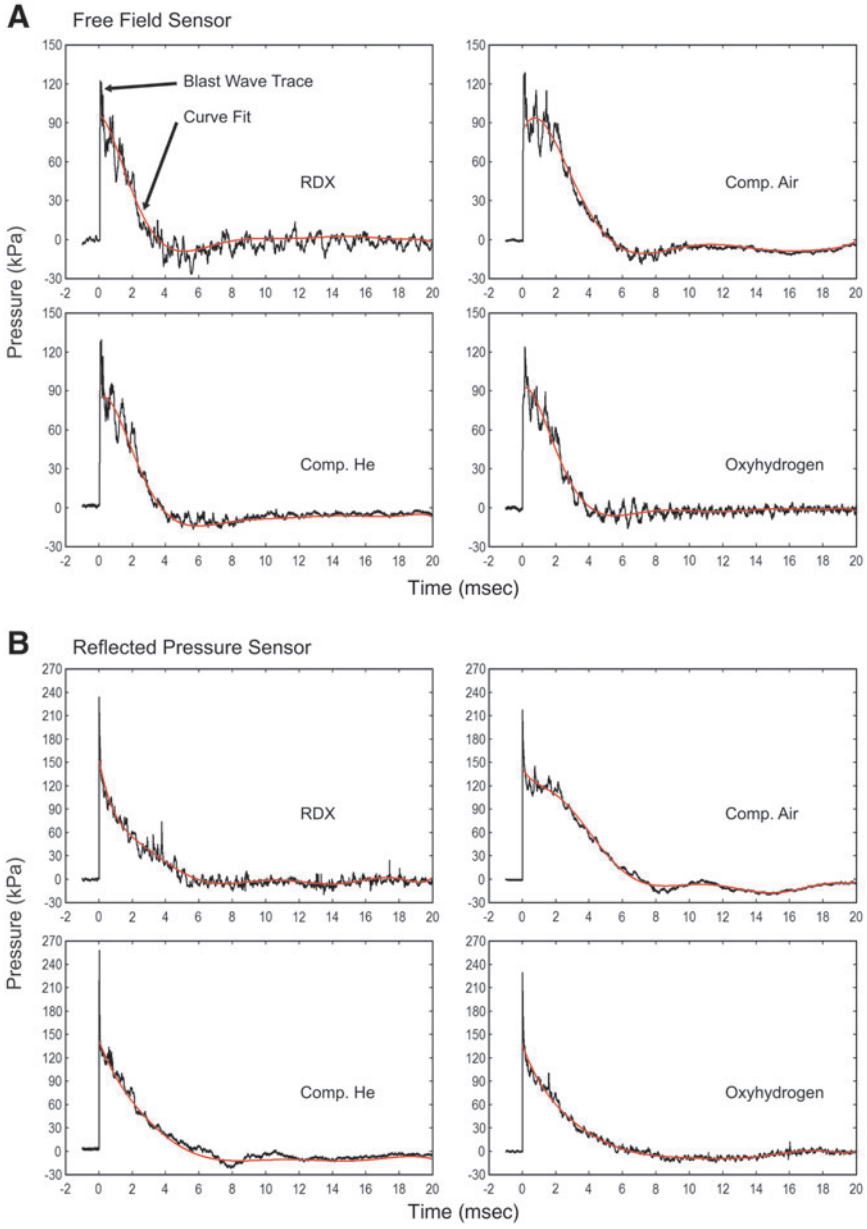

FIG. 3. Representative pressure-time traces are shown for each of the blast modes, with the free-field (side-on) sensor recordings shown in **A**, and reflected (face-on) sensor recordings shown in **B**. Eighth-order curve fits, indicated by a red line, were generated to smooth out the oscillations in the pressure-time traces to enable more accurate estimation of the time points at which the pressure traces crossed below the ambient pressure level (RDX, cyclotrimethylenetrinitramine; Comp. He., compressed helium; Comp. Air., compressed air).

hand-held gas detector (iTX; Industrial Scientific, Oakdale, PA). Immediately following detonation, the gas detector was placed within the MBD so that its sensing element was located where the test animal's head would be. Oxygen and carbon monoxide levels were measured for 30 sec after the detonation, at which point the detector was removed and peak values were recorded.

Animal blast exposure

Male Sprague-Dawley rats were sedated (10 mg/kg diazepam IP) for transport to the blasting site. The rats were transported in individual cages and had access to food and water *ad libitum* throughout the course of the transport. Each cage was maintained in a climate-controlled vehicle until the rat was subjected to blast. Immediately prior to injury, the rats were anesthetized (50 mg/kg sodium pentobarbital IP), fitted with a Kevlar vest designed to protect the thoracic organs (Long et al., 2009), and placed into a mesh netting support (Industrial Netting, Minneapolis, MN), and loaded into the MBD (Fig. 2F) laterally with the left side facing the blast. Once loaded into the MBD, the rat's body was protected by a steel tube that surrounded the body, but left the head exposed to the blast (Fig. 2F). The rats were subjected to compressed air- or oxyhydrogen-driven blasts of 100, 150, or 200 kPa peak overpressure. Two rats were subjected to each condition. The rats were euthanized with an overdose of sodium pentobarbital (150 mg/kg IP) 3 min following the blast. A necropsy was performed on each rat. The thoracic and abdominal organs, including the heart, lungs (including the trachea), liver, spleen, kidneys, bladder, and gastrointestinal tract (the esophagus at the level of the aortic arch through the rectum), were removed, fixed in 10% buffered formalin, and evaluated by a veterinary pathologist. The rat brains were also removed and photographed (Fig. 9) during necropsy. Control rats were euthanized with an overdose of sodium pentobarbital and had their brains removed in the same way as the injured rats. These studies were performed in accordance with a protocol approved by the University of Kentucky Institutional Animal Care and Use Committee (IACUC). This was a preliminary study to determine the blast conditions associated with bTBI, as well as possible damage to other internal organs.

Statistical analysis

A one-way analysis of variance (ANOVA), followed by a Student's Newman-Keuls *post-hoc* analysis, was used to compare the values for each parameter among blast modes. A one-way ANOVA followed by Dunnet's *post-hoc* analysis was used to compare oxygen and carbon monoxide levels to control air. Statistical analyses were performed using the PRISM v4.0 software package (GraphPad Software, San Diego, CA).

Results

Shockwave velocity

The velocity of the shockwave was measured using two sensors, positioned 17 or 18 feet, respectively, from the diaphragm or detonation source. The velocity measured at this distance was approximately 470 m/sec for the RDX, compressed air, and compressed-helium modes, compared to 520 m/sec for oxyhydrogen (Fig. 4).

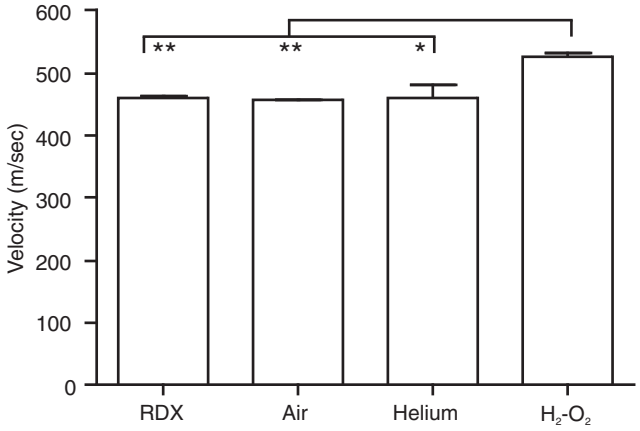

FIG. 4. Shockwave velocity. Shockwave velocity was determined for each mode of the McMillan blast device as described in the methods section. This velocity was slightly greater in oxyhydrogen-driven mode than in the other three modes tested. Error bars represent standard deviation from the mean (*$p < 0.05$, **$p < 0.01$; $n = 3$; RDX, cyclotrimethylenetrinitramine; H_2-O_2, oxyhydrogen).

Positive phase

The blast conditions were adjusted such that the peak positive phase (overpressure) magnitudes, as detected by the free-field sensor, were approximately 120 kPa. These peak overpressures did not differ significantly for each of the four modes examined (Fig. 5A). For the reflected pressure, the maximal overpressure for the RDX-, compressed helium-, and oxyhydrogen-driven modes were similar, and slightly lower for the compressed air-driven mode (Fig. 5A).

Positive phase duration reported by the free-field sensor was significantly shorter with RDX than with compressed air-, compressed helium-, and oxyhydrogen-driven blasts (Fig. 5B). Both compressed helium- and oxyhydrogen-driven blasts had shorter positive durations than compressed air (Fig. 5B). Positive phase durations reported by the reflected pressure sensor were longer than those observed with the free-field sensor, and were significantly greater in duration in both compressed air- and oxyhydrogen-driven blasts than in RDX- and compressed helium-driven blasts (Fig. 5B).

Positive impulses calculated from free-field sensor data were lowest for RDX, slightly greater for compressed helium and oxyhydrogen, and greatest for the compressed air-driven blasts (Fig. 5C). The positive impulses calculated from reflected pressure sensor data taken during compressed air-, compressed helium-, and H_2-O_2-driven blasts, were all higher than those of RDX-driven blasts (Fig. 5C). The overall pattern was largely similar to that observed with the free-field sensor, with the impulse for compressed air being much greater than that observed with the other blast modes, for which compressed helium- was slightly greater than oxyhydrogen- and RDX-driven blast waves (Fig. 5C).

Negative phase

The peak negative phase magnitude detected by the free-field sensor was similar for the RDX, compressed air, and compressed helium modes, but substantially less for oxyhydrogen (Fig. 6). For the reflected pressure sensor, similar

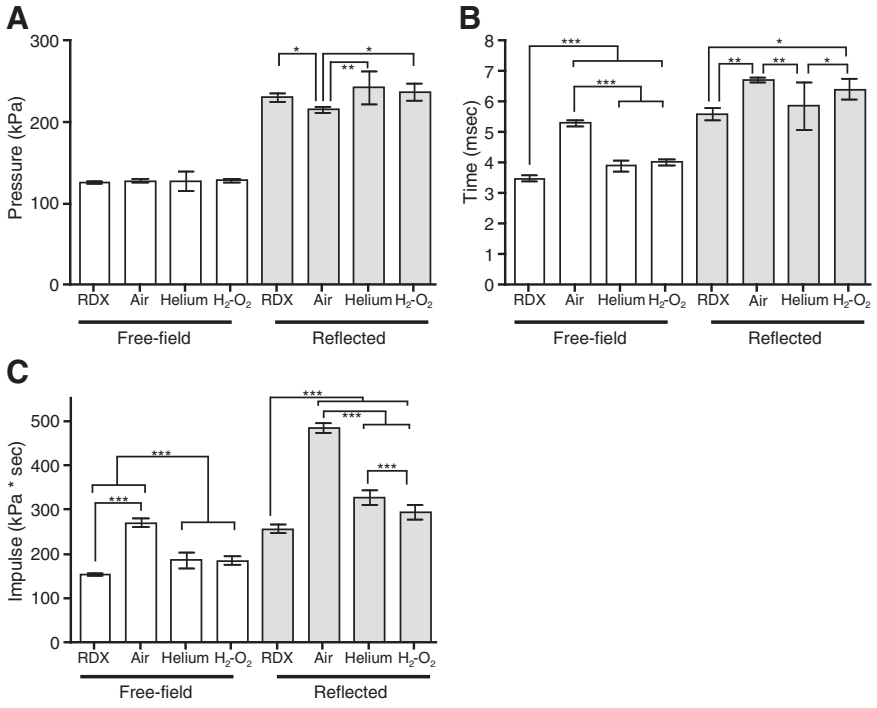

FIG. 5. Properties of the positive phase for each blast mode. (**A**) Mean positive magnitude for both sensors in each blast mode. (**B**) Mean positive phase duration. (**C**) Mean positive impulse. The white bars represent values obtained with the free-field pressure sensor, and the gray bars are values from the reflected pressure sensor. Error bars represent standard deviation from the mean ($*p < 0.05$, $**p < 0.01$, $***p < 0.001$, $n = 6$; RDX, cyclotrimethylenetrinitramine; H_2-O_2, oxyhydrogen).

peak underpressures were observed for RDX, compressed helium, and oxyhydrogen, while the magnitude of the peak negative pressure was much greater with compressed air (Fig. 6).

The duration of the negative phase was difficult to accurately estimate from the pressure-time histograms. The negative phase duration and impulse were therefore not calculated.

Impulse difference

At similar peak overpressures, the difference between the impulses recorded by the reflected and free-field sensors (Benzinger et al., 2009) was greatest for compressed air-driven shockwaves, followed by helium, and were lowest for the oxyhydrogen- and RDX-driven blasts (Fig. 7).

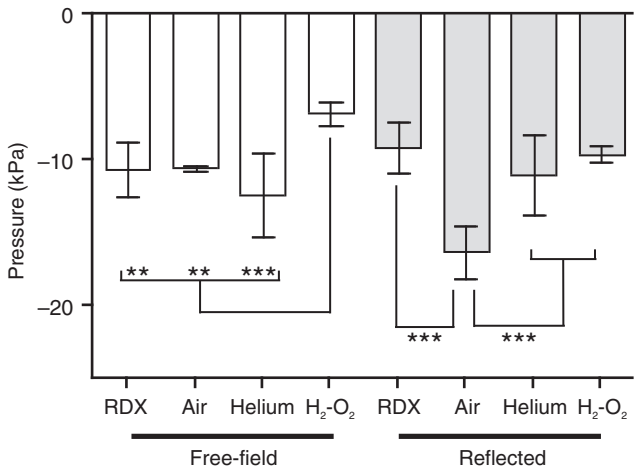

FIG. 6. Negative phase mean peak magnitude for the free-field (white bars) and reflected (gray bars) pressure sensors. Error bars represent standard deviation from the mean ($**p < 0.01$, $***p < 0.001$; $n = 6$; RDX, cyclotrimethylenetrinitramine; H_2-O_2, oxyhydrogen).

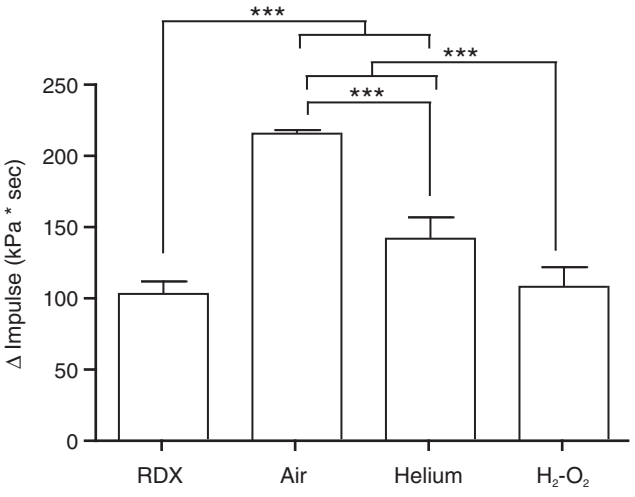

FIG. 7. Impulse difference. The difference in impulse was calculated by subtracting the positive impulse obtained using the free-field sensor from that recorded with the reflected pressure sensor. Error bars represent standard deviation from the mean ($***p < 0.001$, $n = 6$; RDX, cyclotrimethylenetrinitramine; H_2-O_2, oxyhydrogen).

Gas content following blast

Oxygen content was reduced by approximately 75% following helium-driven blasts, and moderately reduced following oxyhydrogen-driven blasts (Fig. 8A). Carbon monoxide content was very high following oxyhydrogen-driven blasts, and above acceptable levels following RDX-driven blasts, although the increase in carbon monoxide levels following RDX-driven blasts was not statistically significant (Fig. 8B). The elevated carbon monoxide levels observed following oxyhydrogen-driven blasts are the result of combustion of the polyethylene bag used to contain the oxyhydrogen gas prior to detonation, as there is no source for carbon in a hydrogen-oxygen condensation reaction. Combustion of polyethylene results in high levels of carbon monoxide (Michal, 1983). Similarly, the slight increase observed following RDX is thought to result from combustion of the latex and electrical tape used to secure the RDX prior to detonation.

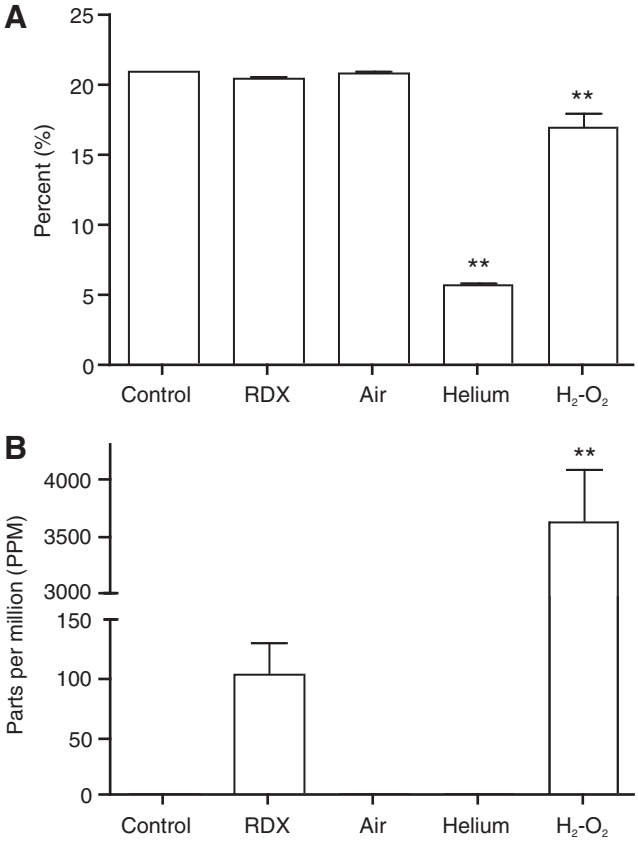

FIG. 8. Gas content following blasts. Oxygen (**A**) and carbon monoxide (**B**) levels within the McMillan blast device were measured following blasts of approximately 120 kPa. There was a substantial decrease in oxygen levels following helium-driven blasts, and a more modest decrease following oxyhydrogen-driven blasts. Carbon monoxide levels were greatly elevated following oxyhydrogen-driven blasts, as a result of combustion of the polyethylene bag used to contain the gases prior to detonation. The slight increase in carbon monoxide seen following RDX-driven blasts was not statistically significant, but is also thought to result from combustion of the latex and electrical tape used to secure the RDX prior to detonation. Error bars represent standard deviation from the mean (**$p < 0.01$, $n = 3$; cyclotrimethylenetrinitramine; H_2-O_2, oxyhydrogen).

Gross brain pathology

The brain surface vessels of rats exposed to 100-kPa peak overpressure shockwaves appear enlarged and more prominent than those observed in a control (non-blast exposed) rat brain (Fig. 9). At 150 kPa blast overpressure the blood vessels appear larger and hematomas are evident. This is even more prominent at 200 kPa. At each blast overpressure level, the external gross brain pathology is more pronounced with compressed air- than with oxyhydrogen-driven blasts (Fig. 9). Necropsy did not reveal blast-related pathology in the thoracic and abdominal organs in any of the treatment groups.

Discussion

Blast-induced TBI in military and civilian populations results from shockwaves produced by high-energy chemical explosives (Elder and Cristian, 2009; Hoge et al., 2008). This can be modeled using chemical explosives in the open field, often with large animals as subjects (Axelsson et al., 2000; Garner et al., 2009; Richmond et al., 1967). Alternatively, shock tubes offer several advantages for investigations of the physiological effects of blasts, particularly with small animals (Celander et al., 1955; Clemedson, 1956). Shock tubes are designed to focus the energy from the blast wave source in a linear direction, thus maximizing the amount of blast energy that impacts the test subject, and decreasing the variability in the blast wave itself. In contrast to free-field explosions, the velocity and pressure of the shockwave does not decay exponentially along the distance of the shock tube (Celander et al., 1955). Also, smaller quantities of explosives are required to produce target peak overpressures (Bauman et al., 2009).

Shock tubes typically consist of a tube in which a high-pressure gas, the driver gas, is separated from a low-pressure gas, the driven gas, by a diaphragm. The diaphragm can be ruptured by the pressure of the driving gas, mechanically, or by an explosive charge using a combustible mixture of gases. Following the rupture of the diaphragm, the resultant pressure waves compress into a shockwave that travels through the driven gas at a supersonic velocity. In the present study the driver gas was compressed air, compressed helium, a mixture of oxygen and hydrogen, or the chemical explosive RDX. The driven gas was atmospheric air.

Compressed air-driven shock tubes have been used to examine the effects of blast waves on small animals since approximately 1949 (Cassen et al., 1950; Clemedson, 1949). By varying the size of the high-pressure chamber, the positive phase duration can be altered for a given maximal overpressure (Celander et al., 1955; Richmond et al., 1968). Air-driven shock tubes are the model most widely used for experimental bTBI studies (Celander et al., 1955; Cernak et al., 2001; Chavko et al., 2007; Elsayed, 1997; Long et al., 2009; Saljo et al., 2009). However, the pressure-time trace from air-driven shock tubes is flatter than the peaked waves resulting from high explosives (Richmond et al., 1968). As a result of the flattening of the peak prior to decay of the shockwave, the duration of the overpressure wave was greater for compressed air than with the other driving modes used in the present study. Also, the peak overpressures attained with compressed air plateau with increasing pressure in the compression chamber

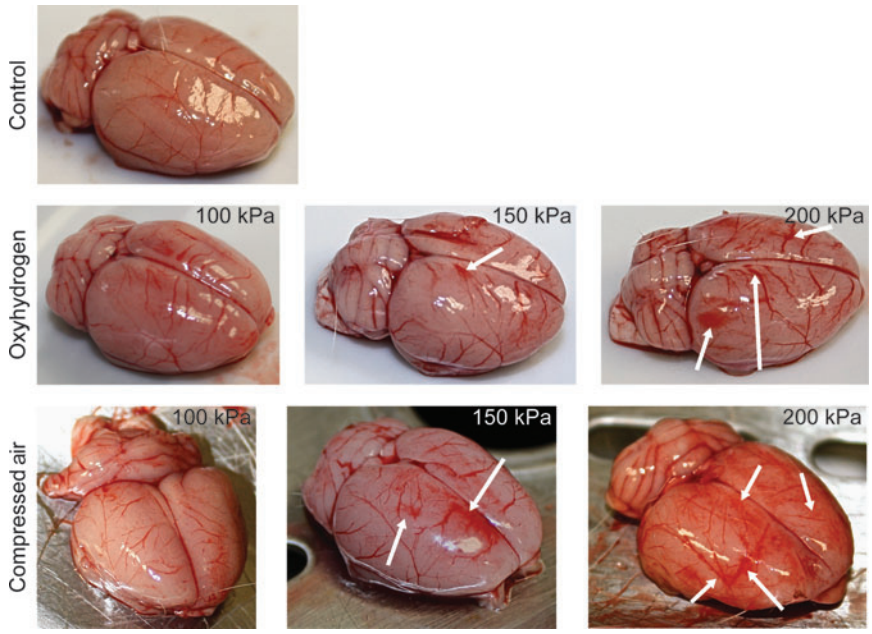

FIG. 9. Gross brain pathology. Representative photographs of the rat brains following exposure of the rats to compressed air-driven and oxyhydrogen-driven blasts of various peak overpressures. Blast exposure resulted in larger blood vessel diameters and hematomas (white arrows), which were more prominent with increasing peak overpressures. The vascular damage was also more prominent with compressed air- compared to oxyhydrogen-driven blasts of similar peak overpressures.

(Celander et al., 1955), making it difficult to achieve a wide range of peak overpressures. In addition, air-driven shock tubes do not model other components of a chemical blast, including acoustic, thermal, optical, and electromagnetic components (Ling et al., 2009). Thus, while compressed air-driven shock tubes are convenient, and certain properties of the resultant shockwave are modifiable, it is also important to recognize the differences in a shockwave resulting from compressed air, compared to that produced by a chemical explosion.

Compressed atmospheric air is a mixture of mostly diatomic nitrogen, followed by diatomic oxygen, and to a much lesser extent, water vapor and other trace gases. Due in part to intermolecular forces strengthened during compression, compressed air fails to expand as quickly as would an ideal gas when the membrane is ruptured. Use of a light gas, such as helium, improves the performance of shock tubes due to the increased speed of sound in helium compared to air, resulting in a lower driver- to driven-tube ratio (Lu and Wilson, 2003; Warren and Harris, 1970). This is consistent with results obtained in the present study, in which helium produced a sharper overpressure peak and shorter overpressure duration compared to compressed air. However, its disadvantages include the expense of helium and the large amounts required to pressurize the driver tube (Lu and Wilson, 2003). Additionally, following shock tube blasts, the driver gas replaces all or part of the driven gas. Oxygen monitoring experiments revealed a 75% reduction in oxygen content within the shock tube following helium-driven blasts.

The variability (standard deviation) of the peak overpressures obtained with helium was greater than that observed for the other blast modes. For compressed air-driven blasts, natural rupture of the Mylar membrane produced a shockwave with a peak overpressure of approximately 120 kPa. To produce a helium-driven shockwave of equal peak overpressure, the Mylar membrane had to be mechanically ruptured at a lower compression chamber pressure. This is because helium, being a lighter gas, expands more rapidly than air following membrane rupture. The greater variability observed in recordings from helium-driven blasts may be due to variations associated with the mechanical rupture of the Mylar membrane at the desired compression chamber pressure.

RDX (cyclotrimethylenetrinitramine) is the major component of plastic explosives widely used by the military and in IEDs (U.S. Army, 1984; Kopp, 2008). Although the use of RDX provides an accurate representation of the chemical explosives encountered in warfare, experimentation with explosive nitroamines, including RDX, is not without significant drawbacks. In addition to the cost of the explosive and detonators consumed in each blast, explosive nitroamines require specialized equipment for their proper transport and use, including explosive storage containers, dynamos or "shot boxes" for detonator ignition, and often a separate transport vehicle. Using explosive nitroamines in the U.S. requires federal licensure that can be costly to obtain, and requires at least 2 years of working experience with explosives to obtain, in addition to individual state requirements. In addition, RDX in its undetonated form is a suspected carcinogen (U.S. Department of Health and Human Services, 1995), and the by-products of RDX detonation contain potent vasodilators similar to glyceryl trinitrate tablets, and thus present a risk of developing a nitric oxide tolerance to personnel who handle it. These disadvantages make RDX unsuitable as a driving source for use in investigations involving small animals.

When detonated, oxyhydrogen undergoes a chemical reaction that yields energy much like an RDX detonation, but the chemical by-product is water vapor. In addition, compressed hydrogen and oxygen can be purchased without a license, stored separately, and are only combined when inside

the MBD. The oxyhydrogen-driven blasts are also relatively inexpensive, as small amounts of oxygen and hydrogen are utilized, and other expenses include the chordite charge (shotgun primer), and a polyethylene bag to contain the gases within the device until detonation. The high carbon monoxide levels seen following oxyhydrogen-driven blasts are likely due to burning of the polyethylene bag. With both the helium- and oxyhydrogen-driven blasts, it is important to remove the experimental animal from the shock tube within a few seconds following blast exposure to prevent the consequences of prolonged exposure to helium or carbon monoxide.

The pressure-time traces produced by oxyhydrogen were similar to those of RDX in many respects. However, oxyhydrogen had a faster average shockwave velocity compared to RDX, compressed air, and helium. This may reflect the heat generated during the oxyhydrogen explosion, which results in greater expansion of the gas, and allows the shockwave to travel faster. Heating of the driving gas is one method used to improve shock tube performance (Lu and Wilson, 2003). Overall, the results demonstrate that the pressure-time traces produced by oxyhydrogen more closely resemble those generated by RDX than those using compressed air and helium.

The blast components that contribute to bTBI are largely unknown. Previous studies have largely focused on the maximal overpressure as the critical factor (Cernak et al., 2001; Chavko et al., 2007; Long et al., 2009; Saljo et al., 2009). However, the peak overpressures used to induce bTBI have varied widely, ranging from 20 kPa to 340 kPa for whole-body exposure in rats (Cernak et al., 2001; Moochhala et al., 2004), 150 kPa for head-only exposure (Cheng et al., 2010), and up to 10,000 kPa for direct brain exposure (Kato et al., 2007). As noted by Ling and associates (2009), the assumption that bTBI is dependent only upon the peak overpressure may not be valid.

Although there is a relationship between peak pressure and lethality in sheep (Richmond et al., 1968), duration of the overpressure phase and the positive impulse (integral of overpressure$\times$duration) are also known to influence the extent of lung injury (Clemedson, 1956). A model of the underpressure component of the blast wave can result in similar lung damage to that produced by overpressure (Zhang et al., 1996). Of particular relevance in the present study is that compressed air differed substantially from the other blast modes in having a greater positive impulse and Δ impulse at similar maximal overpressures. This suggests the possibility that a compressed air-driven shockwave may be more damaging than a chemical explosive-driven shockwave of similar peak overpressure. In the present study, the vascular damage seen on the brain surface was more pronounced following compressed air- compared to oxyhydrogen-driven blasts of similar peak overpressures. The hematomas observed in the present study are consistent with those observed in both military personnel and civilians following blast exposure, and in previous studies utilizing animal models of bTBI (Levi et al., 1990; Murthy et al., 1979; Scott et al., 1986; Svetlov et al., 2010). A more thorough quantitative evaluation of gross and microscopic brain pathology following exposure of rats to the various blast sources is ongoing.

The blast wave components contributing to bTBI are not well understood, but may be quite different from those causing damage to air-filled organs such as the lung (Ling et al., 2009). Using a single blast source, it is difficult to determine the blast wave characteristics that contribute to injury. The MBD can utilize a variety of driving sources (compressed air, compressed helium, oxyhydrogen, and RDX) to produce shock waves of similar maximal overpressure. The results demonstrate that these different blast modes differ substantially in their pressure-time traces at similar peak overpressures, and that these differences may influence the extent of brain injury produced by each blast mode.

Compressed air-driven blasts had a much longer positive duration, impulse, and dynamic energy, compared to the other blast modes, and also resulted in greater vascular damage than oxyhydrogen. Helium-driven shockwaves more closely resembled those produced by RDX, but the replacement of air by helium within the expansion chamber of the shock tube created a hypoxic environment. Oxyhydrogen-driven shockwaves closely resembled those resulting from RDX, but produced high levels of carbon monoxide, resulting from combustion of the polyethylene bag. For both helium- and oxyhydrogen-driven blasts, rapid removal of the animals following blast exposure is necessary to prevent damage resulting from the hypoxic environment within the shock tube. This multi-mode shock tube will enable comparison of the pressure-time signatures produced using each blast mode with the extent of brain injury in small-animal models, facilitating evaluation of the blast wave components contributing to bTBI.

Acknowledgments

D.V.R. was supported by National Institutes of Health (NIH) grant T32DA022738. We would also like to thank GLR Enterprises, L.L.C., for their generous donation of time and materials, without which this work would not have been possible. Additional support was provided by NIH grant P30NS051220.

Author Disclosure Statement

No competing financial interests exist.

References

Armonda, R.A., Bell, R.S., Vo, A.H., Ling, G., DeGraba, T.J., Crandall, B., Ecklund, J., and Campbell, W.W. (2006). Wartime traumatic cerebral vasospasm: recent review of combat casualties. Neurosurgery 59, 1215–1225.

Axelsson, H., Hjelmqvist, H., Medin, A., Persson, J.K., and Suneson, A. (2000). Physiological changes in pigs exposed to a blast wave from a detonating high-explosive charge. Mil. Med. 165, 119–126.

Baker, W.E. (1973). *Explosions in Air*. University of Texas Press: Austin.

Bauman, R.A., Ling, G., Tong, L., Januszkiewicz, A., Agoston, D., Delanerolle, N., Kim, Y., Ritzel, D., Bell, R., Ecklund, J., Armonda, R., Bandak, F., and Parks, S. (2009). An introductory characterization of a combat-casualty-care relevant swine model of closed head injury resulting from exposure to explosive blast. J. Neurotrauma 26, 841–860.

Benzinger, T.L., Brody, D., Cardin, S., Curley, K.C., Mintun, M.A., Mun, S.K., Wong, K.H., and Wrathall, J.R. (2009). Blast-related brain injury: imaging for clinical and research applications: report of the 2008 St. Louis workshop. J. Neurotrauma 26, 2127–2144.

Cassen, B.K., Curtis, L., and Kistler, K. (1950). Initial studies of the effect of laboratory proudced air blast on animals. J. Aviat. Med. 23.

Celander, H., Clemedson, C.J., Ericsson, U.A., and Hultman, H.I. (1955). The use of a compressed air operated shock tube for physiological blast research. Acta Physiol. Scand. 33, 6–13.

Cernak, I., and Noble-Haeusslein, L.J. (2010). Traumatic brain injury: an overview of pathobiology with emphasis on military populations. J. Cereb. Blood Flow Metab. 30, 255–266.

Cernak, I., Wang, Z., Jiang, J., Bian, X., and Savic, J. (2001). Ultrastructural and functional characteristics of blast injury-induced neurotrauma. J. Trauma 50, 695–706.

Chavko, M., Koller, W.A., Prusaczyk, W.K., and McCarron, R.M. (2007). Measurement of blast wave by a miniature fiber optic pressure transducer in the rat brain. J. Neurosci. Methods 159, 277–281.

Chavko, M., Prusaczyk, W.K., and McCarron, R.M. (2006). Lung injury and recovery after exposure to blast overpressure. J. Trauma 61, 933–942.

Cheng, J., Gu, J., Ma, Y., Yang, T., Kuang, Y., Li, B., and Kang, J. (2010). Development of a rat model for studying blast-induced traumatic brain injury. J. Neurol. Sci. 294, 23–28.

Clemedson, C.J. (1949). An experimental study on air blast injuries. Acta Physiol. Scand. 18, Suppl. 61.

Clemedson, C.J. (1956). Blast injury. Physiol. Rev. 36, 336–354.

Elder, G.A., and Cristian, A. (2009). Blast-related mild traumatic brain injury: mechanisms of injury and impact on clinical care. Mt. Sinai J. Med. 76, 111–118.

Elsayed, N.M. (1997). Toxicology of blast overpressure. Toxicology 121, 1–15.

Garner, J.P., Watts, S., Parry, C., Bird, J., and Kirkman, E. (2009). Development of a large animal model for investigating resuscitation after blast and hemorrhage. World J. Surg. 33, 2194–2202.

Gruss, E. (2006). A correction for primary blast injury criteria. J. Trauma 60, 1284–1289.

Hoge, C.W., McGurk, D., Thomas, J.L., Cox, A.L., Engel, C.C., and Castro, C.A. (2008). Mild traumatic brain injury in U.S. soldiers returning from Iraq. N. Engl. J. Med. 358, 453–463.

Kato, K., Fujimura, M., Nakagawa, A., Saito, A., Ohki, T., Takayama, K., and Tominaga, T. (2007). Pressure-dependent effect of shock waves on rat brain: induction of neuronal apoptosis mediated by a caspase-dependent pathway. J. Neurosurg. 106, 667–676.

Kopp, C. (2008). Technology of improvised explosive devices. Defence Today 46–49.

Levi, L., Borovich, B., Guilburd, J.N., Grushkiewicz, I., Lemberger, A., Linn, S., Schachter, I., Zaaroor, M., Braun, J., and Feinsod, M. (1990). Wartime neurosurgical experience in Lebanon, 1982–85. II: Closed craniocerebral injuries. Isr. J. Med. Sci. 26, 555–558.

Ling, G., Bandak, F., Armonda, R., Grant, G., and Ecklund, J. (2009). Explosive blast neurotrauma. J. Neurotrauma 26, 815–825.

Long, J.B., Bentley, T.L., Wessner, K.A., Cerone, C., Sweeney, S., and Bauman, R.A. (2009). Blast overpressure in rats: recreating a battlefield injury in the laboratory. J. Neurotrauma 26, 827–840.

Lu, F.K., and Wilson, D.R. (2003). Detonation driver for enhancing shock tube performance. Shock Waves 12, 457–468.

Marks, M.E. (2002). *The Emergency Responders Guide to Terrorism*. Red Hat Publishing, pps. 30–32.

Mayorga, M.A. (1997). The pathology of primary blast overpressure injury. Toxicology 121, 17–28.

Michal, J. (1983). Combustion products of polymeric materials. 1—Test chamber CAB 4.5. Fire Materials 7, 163–168.

Moochhala, S.M., Md, S., Lu, J., Teng, C.H., and Greengrass, C. (2004). Neuroprotective role of aminoguanidine in behavioral changes after blast injury. J. Trauma 56, 393–403.

Murthy, J.M., Chopra, J.S., and Gulati, D.R. (1979). Subdural hematoma in an adult following a blast injury. Case report. J. Neurosurg. 50, 260–261.

Richmond, D.R., Damon, E.G., Fletcher, E.R., Bowen, I.G., and White, C.S. (1968). The relationship between selected blast-wave parameters and the response of mammals exposed to air blast. Ann. NY Acad. Sci. 152, 103–121.

Richmond, D.R., Damon, E.G., Fletcher, E.R., Bowen, I.G., and White, C.S. (1967). The relationship between selected blast-wave parameters and the response of mammals exposed to air blast. Techn. Progr. Rep. DASA 1860. Fission Prod. Inhal. Proj. 1–36.

Saljo, A., Arrhen, F., Bolouri, H., Mayorga, M., and Hamberger, A. (2008). Neuropathology and pressure in the pig brain resulting from low-impulse noise exposure. J. Neurotrauma 25, 1397–1406.

Saljo, A., Svensson, B., Mayorga, M., Hamberger, A., and Bolouri, H. (2009). Low levels of blast raises intracranial pressure and impairs cognitive function in rats. J. Neurotrauma 26, 1345–1352.

Scott, B.A., Fletcher, J.R., Pulliam, M.W., and Harris, R.D. (1986). The Beirut terrorist bombing. Neurosurgery 18, 107–110.

Svetlov, S.I., Prima, V., Kirk, D.R., Gutierrez, H., Curley, K.C., Hayes, R.L., and Wang, K.K. (2010). Morphologic and biochemical characterization of brain injury in a model of controlled blast overpressure exposure. J. Trauma 69, 795–804.

U.S. Army. (1984). Military Explosives. Department of the Army Technical Manual. Report Number TM 9-1300-214. Washington.

U.S. Department of Health and Human Services. (1995). Toxicological Profile for RDX. Agency for Toxic Substances and Disease Registry. Public Health Service. Atlanta.

Warren, W.R., and Harris, C.J. (1970). A critique of high performance shock tube driving techniques, in: Shock Tubes. *Proc. 7th Int. Shock Tube Symp.*, June 23–25, 1969. I.I. Glass (ed). University of Toronto Press: Toronto, pps. 143–176.

Zhang, J., Wang, Z., Leng, H., and Yang, Z. (1996). Studies on lung injuries caused by blast underpressure. J. Trauma 40, S77–S80.

Address correspondence to:
James W. Geddes, Ph.D.
Spinal Cord and Brain Injury Research Center
B477 Biomedical & Biological Sciences
Research Building (BBSRB)
741 South Limestone Street
University of Kentucky
Lexington, KY 40536-0509

E-mail: jgeddes@uky.edu